JACS
JOURNAL OF THE AMERICAN CHEMICAL SOCIETY
pubs.acs.org/JACS
Article

Concentration- and Solvation-Induced Reversible Structural Transformation and Assembly of Polynuclear Gold(I) Sulfido Complexes

Liang-Liang Yan, Liao-Yuan Yao, and Vivian Wing-Wah Yam*

Cite This: https://dx.doi.org/10.1021/jacs.0c04677
Read Online

ABSTRACT: A series of polynuclear gold(I) sulfido complexes of bis(diphenylphosphino)amine ligands has been synthesized and characterized. A rather small variation in the conformation of the bis(diphenylphosphino)amine ligands has led to distinct differences in the identity of the polynuclear gold(I) sulfido complexes formed. Unprecedented concentration-dependent and solvation-dependent reversible cluster-to-cluster transformation between a dodecanuclear gold(I) sulfido complex (L^{Me}-Au_{12}) and a hexanuclear gold(I) sulfido complex (L^{Me}-Au_6) has been observed. The transformation process has been monitored not only by ^1H and $^{31}P\{^1H\}$ NMR spectroscopy but also by UV−vis absorption spectroscopy and high-resolution electrospray ionization mass spectrometry (HR-ESI-MS) in the solution state. This work has provided a simple approach to achieve structure modulation of gold(I) sulfido complexes and an understanding of supramolecular transformations via external stimuli.

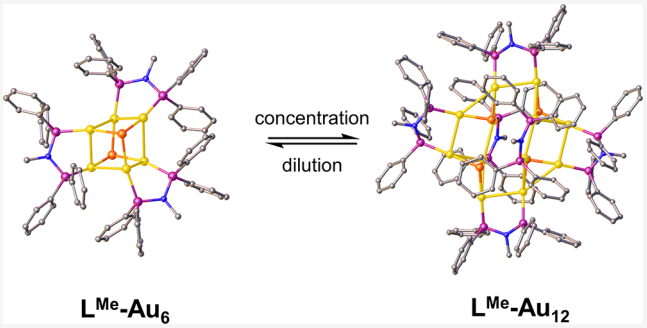

INTRODUCTION

In nature, some fundamental biomacromolecules can spontaneously change their structures through the introduction of external stimuli or changes in the microenvironment, which is usually referred to as "supramolecular transformations".[1] Studying the stimuli-responsive behavior not only can help to uncover the foundation of biological functions but also can enable the design of artificial systems that are capable of changing their properties in response to external physical or chemical stimuli.[1,2] In recent years, there has been a growing interest in the understanding and control of structural transformation and assembly of molecules induced by various stimuli, which are usually associated with the manipulation of noncovalent interactions.[3−7] Metal−ligand coordination bonds have been extensively employed in the construction of stimuli-responsive assemblies owing to their dynamic and reversible features.[1,2,6−17] Polynuclear gold(I) complexes represent an interesting class of metallosupramolecular system based on metal−ligand coordination bonds and gold(I)···gold(I) interactions, the latter of which has been termed aurophilic interaction by Schmidbaur and co-workers.[18−21] This attractive interaction enables the polynuclear gold(I) complexes to possess a variety of configurations and to show rich structure-correlated photophysical properties.[20−48] Apart from modulating the photophysical properties via changes in the structural properties by molecular design, variation in the concentration also represents an effective way to alter and control the process of supramolecular self-assembly and the formation and regulation of supramolecular structures.[1,2,11,49,50] Although there have been reports on concentration-induced isomerization of metal−ligand assemblies,[1,2,10,51,52] similar works have not been explored in the gold(I) sulfido complex system.

The use of monodentate phosphine ligands to construct monolayer-protected gold nanoclusters could be traced back to the 1960s. In 1969, Mason and co-workers first reported the Au_{11} structure, $[Au_{11}(PPh_3)_7(SCN)_3]$, which could be considered as an incomplete icosahedral structure.[53] Mingos and co-workers later reported the icosahedral Au_{13} nanocluster, $[Au_{13}(PMe_2Ph)_{10}Cl_2](PF_6)_3$, by reduction of the gold(I) precursor $[(PMe_2Ph)AuCl]$ with $[Ti(\eta\text{-}C_6H_5Me)_2]$.[54] Teo and co-workers reported the Au_{39} cluster, $[Au_{39}(PPh_3)_{14}Cl_6]Cl_2$, with a hexagonal close-packed layered structure.[55]

Murray and co-workers reported the subnanometer monolayer-protected clusters (MPCs), $[Au_{13}(PPh_3)_4(S(CH_2)_{11}CH_3)_2]Cl_2$ and $[Au_{13}(PPh_3)_4(S(CH_2)_{11}CH_3)_4]$, with mixed ligands by using the dodecanethiolate ligands to replace some of the monodentate phosphine ligands.[56] The monodentate phosphine ligands, such as PPh_3, P^iPr_3, $PMePh_2$, and PMe_3, have also been used to construct the polynuclear gold(I)

Received: April 29, 2020

Scheme 1. Structural Modulation of Gold(I) Sulfido Complexes

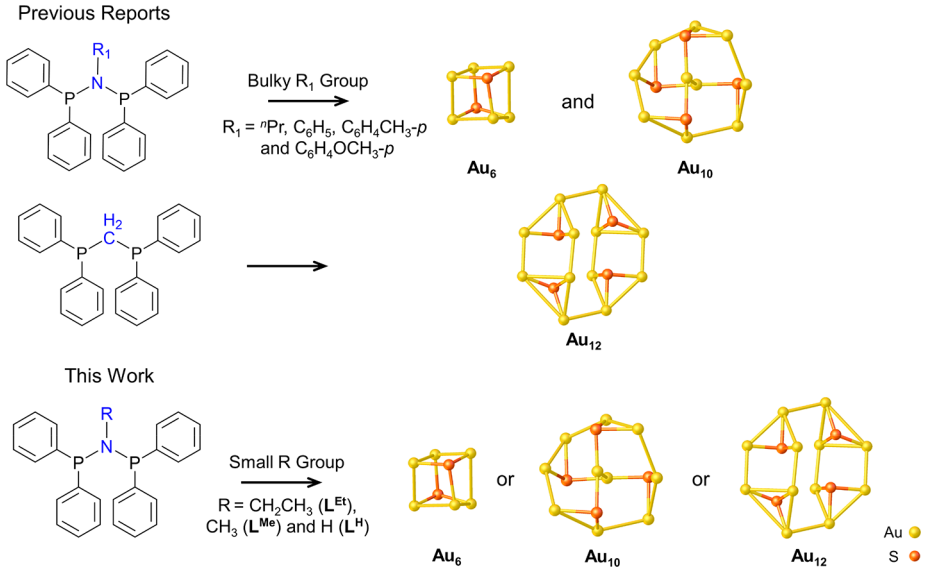

sulfido complexes.[57−59] Since 1999, our group has focused on the design and synthesis of polynuclear gold(I) complexes that are bridged by diphosphine ligands and the μ_3-sulfido ligands.[26,60−65] Polynuclear gold(I) species have emerged to be one of the most prevalent systems in the gold family owing to their relative ease of synthesis and their highly stable nature.[26,60−65] In recent years, our group has demonstrated the interesting phenomenon of polynuclear gold(I)-based cluster-to-cluster transformations.[66−69] However, to the best of our knowledge, to accomplish reversible interconversion between gold(I) sulfido complexes is still a formidable challenge. On the basis of our previous studies, the distances between two phosphorus atoms in the phosphine ligands have been found to play an important role in regulating the structures of gold(I) sulfido complexes. A series of decanuclear and hexanuclear gold(I) sulfido complexes with various bridging bis(diphenylphosphino)amine (PNP) ligands has been successfully accomplished (Scheme 1).[26,60,64,65] However, a dodecanuclear gold(I) sulfido cluster was obtained instead by using bis(diphenylphosphino)methane (dppm) as the ligand,[63] which has a similar P−P distance (~3.1 Å) as PNP ligands (Scheme 1). Given the ready functionalization of the PNP ligand at the amino nitrogen, modification of substituents with different steric effects at the N atom may lead to a control of the nuclearity of the polynuclear gold(I) sulfido complexes. It is envisaged that the steric effect of the R groups on the N atom of the diphosphine ligands is crucial to regulate the bite distance of the bridging ligand and hence the structure of these clusters.

In this work, a series of chlorogold(I) precursors based on bis(diphenylphosphino)amine ligands, $Ph_2PN(R)PPh_2$ (where R = CH_3CH_2 ($\mathbf{L^{Et}}$); R = CH_3 ($\mathbf{L^{Me}}$); R = H ($\mathbf{L^{H}}$)) (Scheme 1) with a systematic decrease in the steric effect, has been employed to synthesize polynuclear gold(I) sulfido complexes. Intriguingly, a systematic decrease in the steric effect of the PNP ligands has dictated the nuclearity of the polynuclear gold(I) sulfido complexes, ranging from decanuclear to dodecanuclear gold(I) sulfido complexes ($\mathbf{L^{Et}}$-$\mathbf{Au_{10}}$, $\mathbf{L^{Me}}$-$\mathbf{Au_{10}}$, $\mathbf{L^{Me}}$-$\mathbf{Au_{12}}$, and $\mathbf{L^{H}}$-$\mathbf{Au_{12}}$). For $\mathbf{L^{Me}}$, a mixture of both the decanuclear and the dodecanuclear gold(I) sulfido complexes ($\mathbf{L^{Me}}$-$\mathbf{Au_{10}}$ and $\mathbf{L^{Me}}$-$\mathbf{Au_{12}}$) was clearly observed in the solid state. Moreover, one of the dodecanuclear gold(I) sulfido complexes ($\mathbf{L^{Me}}$-$\mathbf{Au_{12}}$) shows reversible concentration-modulated interconversion cluster-to-cluster transformation, the process of which has been monitored by ^{1}H NMR, $^{31}P\{^1H\}$ NMR, and high-resolution electrospray ionization mass spectrometry (HR-ESI-MS). The present work demonstrates that a fine-tuning of the steric effect of the ligand can have a significant impact on the regulation of the structure of gold(I) sulfido complexes.

RESULTS AND DISCUSSION

Synthesis, Characterization, and Structure Determination. Reaction of $[Au_2Cl_2(\mathbf{L^{Et}})]$ with H_2S in dichloromethane−pyridine led to a lucid yellow solution that afforded a yellow−green solid after evaporation. Yellow−green block crystals of $\mathbf{L^{Et}}$-$\mathbf{Au_{10}}$ were obtained by slow vapor diffusion of diethyl ether into its dichloromethane solution in 2 weeks. The $^{31}P\{^1H\}$ NMR spectrum of the yellow−green crystals in $CDCl_3$ showed a pair of doublets at δ = 84.56 and 81.69 ppm (Figure S2), which is very similar to those observed for the previously reported propeller-like structures of Au_{10} clusters.[64,66] HR-ESI-MS analyses revealed a molecular ion peak at m/z = 1875.5584 (Figure S3), corresponding to the molecular ion $[Au_{10}(\mathbf{L^{Et}})_4(\mu_3\text{-}S)_4]^{2+}$ ($[\mathbf{L^{Et}}\text{-}\mathbf{Au_{10}}]^{2+}$). The formation of $[Au_{10}(\mathbf{L^{Et}})_4(\mu_3\text{-}S)_4Cl_2]$ has been further confirmed by single-crystal X-ray diffraction studies. Complex $\mathbf{L^{Et}}$-$\mathbf{Au_{10}}$ crystallizes in the tetragonal $P\bar{4}2_1c$ space group. The complex cation adopts a propeller-shaped structure, with a gold macrocycle containing eight gold atoms with a digold unit at the core, bridged by four PNP ligands and four sulfur atoms (Figures 1a and S4). The structure possesses an S_4 point group, which is the same as the previously reported Au_{10} clusters with PNP ligands.[26,64] Intramolecular Au(I)···Au(I) distances are in the range of 2.98−3.33 Å (Table S2), comparable to those reported in other gold(I) μ_3-sulfido complexes.[62−64,66−70]

Reaction of $[Au_2Cl_2(\mathbf{L^{Me}})]$ with H_2S in dichloromethane−pyridine also led to a clear yellow solution. However, two kinds of yellow−green crystals with different morphologies were obtained at different stages by vapor diffusion of diethyl ether into the dichloromethane solution. Yellow−green rectangular

https://dx.doi.org/10.1021/jacs.0c04677
J. Am. Chem. Soc. XXXX, XXX, XXX−XXX

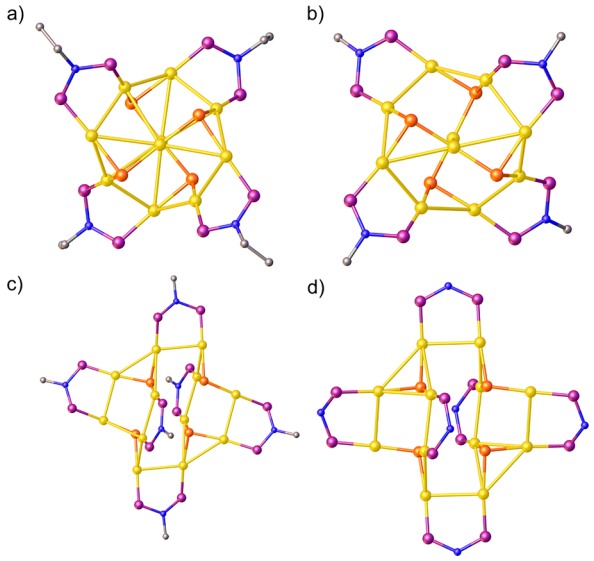

Figure 1. Crystal structures of cluster cations of (a) $\mathbf{L^{Et}}$-$\mathbf{Au_{10}}$, (b) $\mathbf{L^{Me}}$-$\mathbf{Au_{10}}$, (c) $\mathbf{L^{Me}}$-$\mathbf{Au_{12}}$, and (d) $\mathbf{L^{H}}$-$\mathbf{Au_{12}}$. Phenyl rings, counteranions, and hydrogen atoms are omitted for clarity (gray, C; blue, N; purple, P; yellow, Au; orange, S).

crystals ($\mathbf{L^{Me}}$-$\mathbf{Au_{12}}$) are obtained at an earlier stage than the yellow–green block crystals ($\mathbf{L^{Me}}$-$\mathbf{Au_{10}}$). The crystal structures of complexes $\mathbf{L^{Me}}$-$\mathbf{Au_{10}}$ and $\mathbf{L^{Me}}$-$\mathbf{Au_{12}}$ were confirmed by X-ray single-crystal diffraction studies. Complex $\mathbf{L^{Me}}$-$\mathbf{Au_{10}}$ crystallizes in the monoclinic $P2/n$ space group and also adopts a propeller-like Au_{10} cluster structure (Figures 1b and S5). However, complex $\mathbf{L^{Me}}$-$\mathbf{Au_{12}}$ crystallizes in the triclinic $P\bar{1}$ space group and consists of two ship-type Au_6 units bridged by six PNP ligands and four μ_3-sulfido atoms to give a metallamacrobicyclic structure, similar to the previously reported Au_{12} clusters based on the dppm ligand (Figures 1c and S6).[63] Short intramolecular Au(I)···Au(I) distances in the range of 2.92–3.28 Å (Tables S5 and S8) are suggestive of the presence of aurophilic interactions for complexes $\mathbf{L^{Me}}$-$\mathbf{Au_{10}}$ and $\mathbf{L^{Me}}$-$\mathbf{Au_{12}}$.

Unlike the studies where reactions of H_2S with chlorogold(I) precursors would give rise to clear yellow solutions in a dichloromethane–pyridine system, the reaction of $[Au_2Cl_2(\mathbf{L^{H}})]$ with H_2S in the same solvent system led to a yellow–green precipitate, which could be dissolved by adding methanol to the reaction medium. Pale yellow–green block crystals of $\mathbf{L^{H}}$-$\mathbf{Au_{12}}$ were isolated by vapor diffusion of diethyl ether into its methanol solution. HR-ESI-MS analyses confirmed that the molecular ion peak at m/z = 1201.0350 (Figure S7) corresponds to the molecular ion $[Au_{12}(\mathbf{L^{H}})_6(\mu_3\text{-}S)_4]^{4+}$ ($[\mathbf{L^{H}}\text{-}\mathbf{Au_{12}}]^{4+}$). The formation of the $[Au_{12}(\mathbf{L^{H}})_6(\mu_3\text{-}S)_4]Cl_4$ structure was further confirmed by single-crystal X-ray diffraction studies. Complex $\mathbf{L^{H}}$-$\mathbf{Au_{12}}$ crystallizes in the monoclinic $P2_1/c$ space group. There are four Au_3S units surrounded by six PNP ligands to form a metallamacrobicyclic structure (Figures 1d and S8). The majority of Au···Au distances in complex $\mathbf{L^{H}}$-$\mathbf{Au_{12}}$ lie in the range of 2.97–3.37 Å (Table S11), suggesting remarkable intramolecular Au···Au interactions. However, the $^{31}P\{^1H\}$ NMR spectrum of the pale yellow–green crystals in CD_3OD shows three singlets with the same integral ratio at δ = 68.49, 70.36, and 70.65 ppm (Figure S10) rather than two singlets in a ratio of 1:2 reported in a similar metallamacrobicyclic Au_{12} structure based on dppm ligands.[63] The presence of a local C_{2h} symmetry in the solution state may be the reason for the presence of three kinds of chemical environments for the P atoms.

It is worth noting that, when the steric effect decreases from ethyl to methyl on the PNP ligand, a mixture of decanuclear and dodecanuclear gold(I) μ_3-sulfido complexes is obtained. To our knowledge, this is the first example of isolating both the decanuclear and dodecanuclear gold(I) complexes in one pot, which is different from the isolation of a mixture of hexanuclear and decanuclear gold(I) complexes as in the past,[26] possibly proceeding via a different mechanism. In addition, only the dodecanuclear gold(I) μ_3-sulfido complex is observed when the steric effect is further decreased from methyl to hydrogen on the PNP ligand. These results establish the important role of the substituent on the N atom of the diphosphine ligands in controlling the nuclearity of the polynuclear gold(I) sulfido complexes.

Photophysical Studies. Because complexes $\mathbf{L^{Et}}$-$\mathbf{Au_{10}}$ and $\mathbf{L^{Me}}$-$\mathbf{Au_{10}}$ have the same Au_{10} core, the electronic absorption data for complexes $\mathbf{L^{Et}}$-$\mathbf{Au_{10}}$ and $\mathbf{L^{Me}}$-$\mathbf{Au_{10}}$ in methanol at 298 K show similar absorption patterns with the low-energy absorption shoulders at around 400 nm (Figure 2a), which are tentatively assigned as ligand-to-metal charge transfer (LMCT; S → Au) transitions modified by Au(I)···Au(I) interactions.

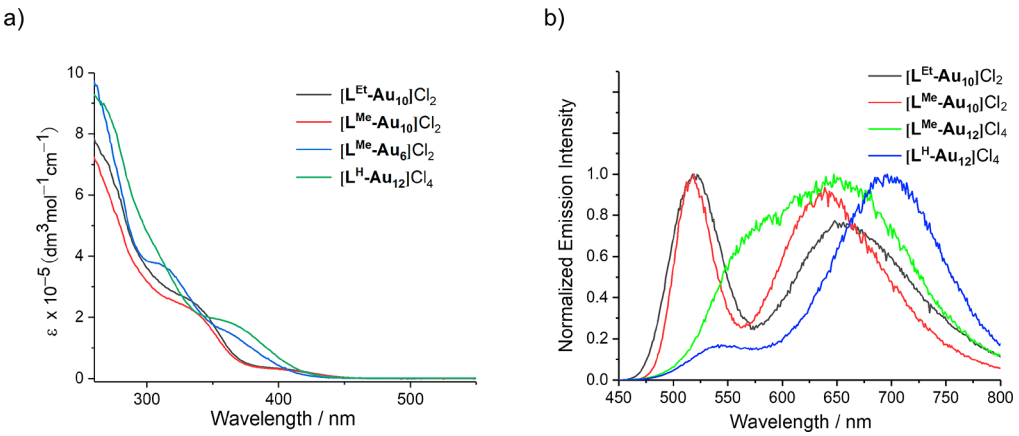

Figure 2. (a) UV–vis spectra of $[\mathbf{L^{Et}}\text{-}\mathbf{Au_{10}}]Cl_2$, $[\mathbf{L^{Me}}\text{-}\mathbf{Au_{10}}]Cl_2$, $[\mathbf{L^{Me}}\text{-}\mathbf{Au_6}]Cl_2$ (obtained from the transformation of $[\mathbf{L^{Me}}\text{-}\mathbf{Au_{12}}]Cl_4$ to $[\mathbf{L^{Me}}\text{-}\mathbf{Au_6}]Cl_2$ in solution state at 10^{-5} M concentration), and $[\mathbf{L^{H}}\text{-}\mathbf{Au_{12}}]Cl_4$ in methanol. (b) Normalized solid-state emission spectra of $[\mathbf{L^{Et}}\text{-}\mathbf{Au_{10}}]Cl_2$, $[\mathbf{L^{Me}}\text{-}\mathbf{Au_{10}}]Cl_2$, $[\mathbf{L^{Me}}\text{-}\mathbf{Au_{12}}]Cl_4$, and $[\mathbf{L^{H}}\text{-}\mathbf{Au_{12}}]Cl_4$ at 77 K.

https://dx.doi.org/10.1021/jacs.0c04677
J. Am. Chem. Soc. XXXX, XXX, XXX–XXX

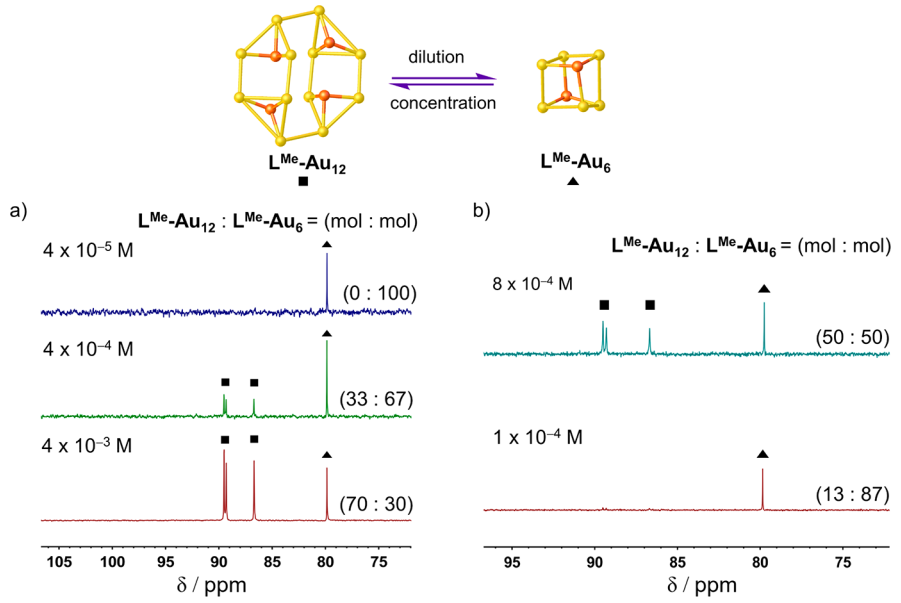

Figure 3. $^{31}P\{^{1}H\}$ NMR spectral changes by (a) varying the initial concentration of $\mathbf{L^{Me}}$-$\mathbf{Au_{12}}$ from 4×10^{-3} to 4×10^{-5} M and (b) increasing the concentration of $\mathbf{L^{Me}}$-$\mathbf{Au_{12}}$ from 1×10^{-4} to 8×10^{-4} M in CD_3OD.

However, complex $\mathbf{L^{H}}$-$\mathbf{Au_{12}}$ shows a different UV−vis absorption spectrum in methanol at 298 K with a low-energy absorption shoulder at around 370 nm (Figure 2a). Excitation of these complexes in the solid state at 77 K results in a dual green and orange−red luminescence. The high-energy emission in the green region is attributed to the metal-perturbed ligand-centered phosphorescence, while the low-energy emission in the orange−red region is assigned to originate from a triplet ligand-to-metal charge-transfer excited state (^{3}LMCT) modified by metal···metal interactions, as suggested from previous studies (Figure 2b).[26]

Concentration-Dependent Reversible Cluster Transformation between $\mathbf{L^{Me}}$-$\mathbf{Au_6}$ and $\mathbf{L^{Me}}$-$\mathbf{Au_{12}}$. The $^{31}P\{^{1}H\}$ NMR spectrum of the yellow−green crystals of complex $\mathbf{L^{Me}}$-$\mathbf{Au_{12}}$ in CD_3OD (6×10^{-4} M) unexpectedly showed three singlets with the same integral ratio at δ = 86.7, 89.3, and 89.5 ppm and a more intense singlet signal at δ = 79.8 ppm, indicating the coexistence of $\mathbf{L^{Me}}$-$\mathbf{Au_{12}}$ and a new species $\mathbf{L^{Me}}$-$\mathbf{Au_6}$ in deuterated methanol solution (Figure S13). According to the $^{31}P\{^{1}H\}$ NMR, HR-ESI-MS, and previous studies (Figures S13 and S14),[26] the structure of $\mathbf{L^{Me}}$-$\mathbf{Au_6}$ ($[Au_6(\mathbf{L^{Me}})_3(\mu_3\text{-}S)_2]^{2+}$) was identified as a hexanuclear complex with a distorted heterocubane core (Scheme 1). Upon dissolution of $\mathbf{L^{Me}}$-$\mathbf{Au_{12}}$, a rather rapid structural transformation from $\mathbf{L^{Me}}$-$\mathbf{Au_{12}}$ to $\mathbf{L^{Me}}$-$\mathbf{Au_6}$ is observed at room temperature. To provide insights into the cluster transformation process, $\mathbf{L^{Me}}$-$\mathbf{Au_{12}}$ (1.6×10^{-3} M) was dissolved in CD_3OD at low temperature, and the NMR experiments were also performed at low temperature (Figures S15 and S16). Variable-temperature $^{31}P\{^{1}H\}$ NMR spectral changes have been monitored from 238 to 298 K (Figure S16). The $^{31}P\{^{1}H\}$ NMR spectrum at 238 K shows three singlets with the same integral ratio at δ = 85.9, 88.3, and 88.8 ppm, unambiguously confirming the sole existence of $\mathbf{L^{Me}}$-$\mathbf{Au_{12}}$ in methanol solution. As the temperature is increased from 238 to 273 K, signals characteristic of $\mathbf{L^{Me}}$-$\mathbf{Au_{12}}$ are downfield-shifted to δ = 86.3, 89.0, and 89.2 ppm, while new signals at around δ = 79.4 ppm attributed to the $\mathbf{L^{Me}}$-$\mathbf{Au_6}$ complex emerge, indicating the conversion of $\mathbf{L^{Me}}$-$\mathbf{Au_{12}}$, which exists as a dodecanuclear species, to a new hexanuclear species ($\mathbf{L^{Me}}$-$\mathbf{Au_6}$). As the temperature is further increased to 298 K, signals characteristic of $\mathbf{L^{Me}}$-$\mathbf{Au_{12}}$ drop in intensity while those of $\mathbf{L^{Me}}$-$\mathbf{Au_6}$ increase, indicating that more $\mathbf{L^{Me}}$-$\mathbf{Au_{12}}$ has been transformed to $\mathbf{L^{Me}}$-$\mathbf{Au_6}$. However, HR-ESI-MS data obtained under more dilute conditions (10^{-7} M) only indicated the existence of $\mathbf{L^{Me}}$-$\mathbf{Au_6}$ (Figure S14). It is likely that the concentration of complex $\mathbf{L^{Me}}$-$\mathbf{Au_{12}}$ in methanol may have an influence on the core structures of these gold(I) sulfido clusters. A concentration-dependent NMR study was undertaken, with the concentration-triggered cluster transformation process monitored by ^{1}H NMR and $^{31}P\{^{1}H\}$ NMR spectral changes under various initial concentrations of $\mathbf{L^{Me}}$-$\mathbf{Au_{12}}$ from 4×10^{-3} to 4×10^{-5} M in CD_3OD (Figures S17 and 3a). Indeed, higher ratios of $\mathbf{L^{Me}}$-$\mathbf{Au_6}$ are obtained from the solution of $\mathbf{L^{Me}}$-$\mathbf{Au_{12}}$ with a lower initial concentration. When the initial concentration of $\mathbf{L^{Me}}$-$\mathbf{Au_{12}}$ is reduced to 4×10^{-5} M, $\mathbf{L^{Me}}$-$\mathbf{Au_6}$ emerged as the sole product, implying that $\mathbf{L^{Me}}$-$\mathbf{Au_{12}}$ has almost been completely transformed to $\mathbf{L^{Me}}$-$\mathbf{Au_6}$ (Figures S17 and 3a). Similarly, only $\mathbf{L^{Me}}$-$\mathbf{Au_6}$ is observed in the HR-ESI-MS of $\mathbf{L^{Me}}$-$\mathbf{Au_{12}}$ in methanol solution (Figure S14) at concentrations lower than 4×10^{-5} M, which further confirms the NMR observation. In addition, $\mathbf{L^{Me}}$-$\mathbf{Au_6}$ is found to convert back to $\mathbf{L^{Me}}$-$\mathbf{Au_{12}}$ upon increasing the concentration. When the concentration is increased from 1×10^{-4} to 8×10^{-4} M by evaporating the CD_3OD under reduced pressure with no heating, a reversible transformation from $\mathbf{L^{Me}}$-$\mathbf{Au_6}$ to $\mathbf{L^{Me}}$-$\mathbf{Au_{12}}$ is found to occur (Figure 3b). In addition, when the chloride counterions are replaced by hexafluorophosphate ions (Figure S18), $[\mathbf{L^{Me}}\text{-}\mathbf{Au_{12}}](PF_6)_4$ also shows concentration-dependent reversible cluster-to-cluster transformation in CD_3CN. Furthermore, $[\mathbf{L^{Me}}\text{-}\mathbf{Au_{12}}](PF_6)_4$ is found to be stable for over 5 successive dilution−concentration cycles (Figure S19), suggestive of the highly reversible cluster-to-cluster transformation processes induced by concentration-switching. On the basis of these results, it can be established that the concentration of $\mathbf{L^{Me}}$-$\mathbf{Au_{12}}$ plays a crucial role in modulating the cluster-to-cluster transformation. This represents the first example of the reversible transformation between two clusters simply by

https://dx.doi.org/10.1021/jacs.0c04677
J. Am. Chem. Soc. XXXX, XXX, XXX−XXX

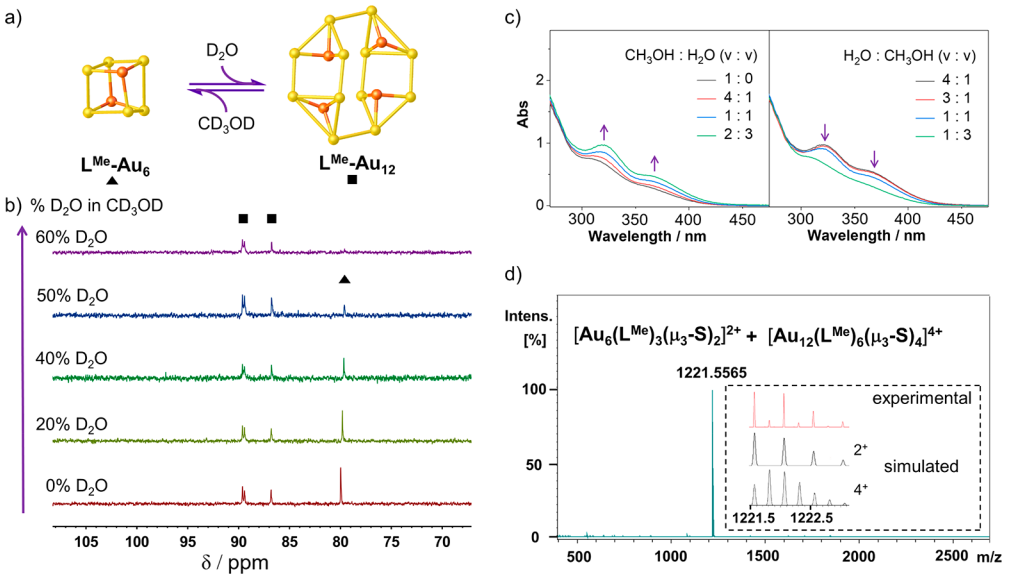

Figure 4. (a) Reversible structural conversion between $\mathbf{L^{Me}}$-$\mathbf{Au_6}$ and $\mathbf{L^{Me}}$-$\mathbf{Au_{12}}$. (b) $^{31}P\{^1H\}$ NMR spectra demonstrating the structural conversion from $\mathbf{L^{Me}}$-$\mathbf{Au_6}$ to $\mathbf{L^{Me}}$-$\mathbf{Au_{12}}$ upon addition of D_2O to a sample solution of CD_3OD. (c) UV−vis spectral changes upon decreasing (left) and increasing (right) the volume ratio of CH_3OH to H_2O. (d) HR-ESI-mass spectrum of complex $\mathbf{L^{Me}}$-$\mathbf{Au_{12}}$ in a solvent mixture of CH_3OH and H_2O.

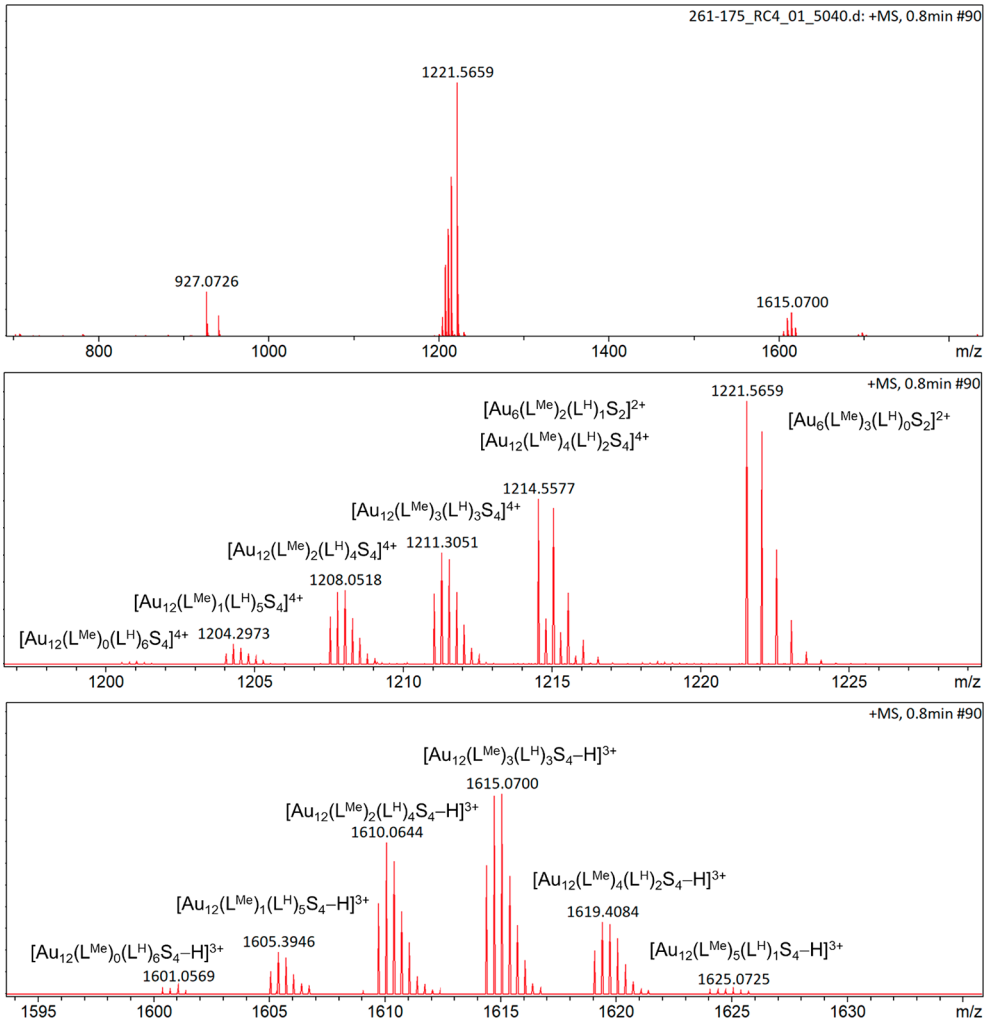

Figure 5. HR-ESI-mass spectra of $\mathbf{L^{Me}}$-$\mathbf{Au_{12}}$ (2×10^{-4} mol) mixed with 1 equiv of $\mathbf{L^{H}}$-$\mathbf{Au_{12}}$ in CH_3OH solution.

https://dx.doi.org/10.1021/jacs.0c04677
J. Am. Chem. Soc. XXXX, XXX, XXX−XXX

changing the concentration of the gold(I) sulfido complex under mild conditions.

To provide insights into the concentration-dependent cluster transformation process, the interconversion between $\mathbf{L^{Me}}$-$\mathbf{Au_6}$ and $\mathbf{L^{Me}}$-$\mathbf{Au_{12}}$ has also been explored by reducing the solvation by addition of bad solvents to force the complexes into closer proximity (Figure 4a). Addition of D_2O to the solution of $\mathbf{L^{Me}}$-$\mathbf{Au_{12}}$ with the initial concentration at around 5×10^{-4} M in CD_3OD has been monitored by $^{31}P\{^1H\}$ NMR spectroscopy (Figure 4b). Upon increasing the content of D_2O, $^{31}P\{^1H\}$ NMR signals characteristic of $\mathbf{L^{Me}}$-$\mathbf{Au_6}$ are found to decrease while those of $\mathbf{L^{Me}}$-$\mathbf{Au_{12}}$ increase. Finally, at a volume ratio of CD_3OD to D_2O of 5:3, $\mathbf{L^{Me}}$-$\mathbf{Au_6}$ has almost been completely converted to $\mathbf{L^{Me}}$-$\mathbf{Au_{12}}$ (Figure 4b). Furthermore, the opposite transformation process can be observed after decreasing the ratio of D_2O by adding more CD_3OD to the solvent mixture of CD_3OD and D_2O (Figure S20). Further supporting evidence comes from the UV−vis absorption spectral changes (Figure 4c) and HR-ESI-MS data in mixed solvents (Figures 4d and S21). The absorption shoulder at around 300−400 nm is found to rise dramatically by increasing the ratio of H_2O (Figure 4c), indicating the transformation of the complexes in solution from $\mathbf{L^{Me}}$-$\mathbf{Au_6}$ to $\mathbf{L^{Me}}$-$\mathbf{Au_{12}}$. Similarly, the opposite transformation process can also be observed by increasing the ratio of CH_3OH (Figure 4c). The molecular ion peak at m/z = 1221.5565 (Figures 4d and S21), corresponding to the molecular ion $[Au_{12}(\mathbf{L^{Me}})_6(\mu_3\text{-}S)_4]^{4+}$ mixed with $[Au_6(\mathbf{L^{Me}})_3(\mu_3\text{-}S)_2]^{2+}$, also indicates the transformation between $\mathbf{L^{Me}}$-$\mathbf{Au_{12}}$ and $\mathbf{L^{Me}}$-$\mathbf{Au_6}$ in mixed solvents.

On the basis of these results, it can be further confirmed that $\mathbf{L^{Me}}$-$\mathbf{Au_{12}}$ shows a concentration-dependent reversible transformation process from its dodecanuclear structure to $\mathbf{L^{Me}}$-$\mathbf{Au_6}$ of a hexanuclear structure in the solution state. Owing to the dynamic nature and the reversibility of aurophilic interactions and Au(I)-S coordination bonds, gold(I) sulfido clusters show their capability of transformation in the solution state. As soon as the metastable $\mathbf{L^{Me}}$-$\mathbf{Au_{12}}$ is dissolved in CH_3OH, a dynamic equilibrium between $\mathbf{L^{Me}}$-$\mathbf{Au_{12}}$ and $\mathbf{L^{Me}}$-$\mathbf{Au_6}$ emerges. The $\mathbf{L^{Me}}$-$\mathbf{Au_{12}}$ complex is found to be more stable at higher concentrations and undergoes transformation to $\mathbf{L^{Me}}$-$\mathbf{Au_6}$ with dilution. The change of solvent conditions is believed to affect the stability and solvation of the polynuclear gold(I) sulfido complexes, which will govern the reversible transformation process.

On the basis of our previous works on gold(I) sulfido clusters,[67,68] which show the dynamic nature of gold(I) sulfido clusters in solution state, it is likely that the transformation between $\mathbf{L^{Me}}$-$\mathbf{Au_6}$ and $\mathbf{L^{Me}}$-$\mathbf{Au_{12}}$ involves changes not only at the core of the clusters but also at the surface of the clusters. To investigate the mechanism of structural conversion between these two clusters, $\mathbf{L^{H}}$-$\mathbf{Au_{12}}$ (2×10^{-4} mol), which does not undergo transformation in CD_3OD, is mixed with 1 equiv of $\mathbf{L^{Me}}$-$\mathbf{Au_{12}}$ in CD_3OD. The $^{31}P\{^1H\}$ NMR spectrum of the mixture shows the formation of an intricate mixture of complexes, consisting of statistical distributions of $[Au_{12}(L^H)_n(L^{Me})_{6-n}S_4]^{4+}$ (n = 0−6) and $[Au_6(L^H)_m(L^{Me})_{3-m}S_2]^{2+}$ (m = 0−3) species (Figure S22). Further identification of the mixtures has been proved by HR-ESI-mass spectral studies. A number of peaks corresponding to multiply charged Au_6 or Au_{12} molecular ions of different bridging ligands are seen (Figure 5). We speculate that the cluster-to-cluster transformation between $\mathbf{L^{Me}}$-$\mathbf{Au_{12}}$ and $\mathbf{L^{H}}$-$\mathbf{Au_{12}}$ may proceed via two possible conversion paths. In one path, the clusters would undergo dissociation, followed by rearrangement and reorganization. In another path, the process involves ligand exchange on the surface of the clusters. A control experiment involving the mixing of $\mathbf{L^{Me}}$-$\mathbf{Au_{12}}$ (2×10^{-4} mol) with 6 equiv of free $\mathbf{L^{H}}$ does not lead to similar observations, but instead some precipitates are formed. HR-ESI-mass spectra further confirm the lack of $[Au_{12}(L^H)_n(L^{Me})_{6-n}S_4]^{4+}$ (n = 0−6) and $[Au_6(L^H)_m(L^{Me})_{3-m}S_2]^{2+}$ (m = 0−3) species in the supernatant (Figure S23). Therefore, the cluster-to-cluster transformation between $\mathbf{L^{Me}}$-$\mathbf{Au_{12}}$ and $\mathbf{L^{H}}$-$\mathbf{Au_{12}}$ may involve initial dissociation, followed by a rearrangement and reorganization process upon mixing, instead of ligand exchange. In addition, the cryospray-ionization-mass spectroscopy (CSI-MS) study of $\mathbf{L^{Me}}$-$\mathbf{Au_{12}}$ in CH_3OH solution shows not only the signal of $\mathbf{L^{Me}}$-$\mathbf{Au_6}$ and $\mathbf{L^{Me}}$-$\mathbf{Au_{12}}$ but also the signal of the $[Au_3(L^{Me})_2S]^+$ ($\mathbf{L^{Me}}$-$\mathbf{Au_3}$) fragment (Figure S24), which is not detectable in NMR spectroscopy (Figure S13). It is likely that the structural conversion between $\mathbf{L^{Me}}$-$\mathbf{Au_{12}}$ and $\mathbf{L^{Me}}$-$\mathbf{Au_6}$ proceeds via dynamic dissociation and reorganization processes involving a transient $\mathbf{L^{Me}}$-$\mathbf{Au_3}$ species that is too short-lived to be observable in the NMR spectra.

However, $\mathbf{L^{Me}}$-$\mathbf{Au_{10}}$ of the same bridging ligand $\mathbf{L^{Me}}$ does not yield a similar cluster transformation phenomenon. The $^{31}P\{^1H\}$ NMR spectrum and HR-ESI-MS data of $\mathbf{L^{Me}}$-$\mathbf{Au_{10}}$ show the sole existence of a Au_{10} cluster without detection of any traces of other clusters (Figures S26 and S27). On the basis of these results, it is envisaged that $\mathbf{L^{Me}}$-$\mathbf{Au_{10}}$ once formed would be thermodynamically stable and would not undergo further transformation to other species even under high dilution.

CONCLUSION

In summary, a small variation in the conformation of bis(diphenylphosphino)amine ligands has led to rather distinct changes in the structure of the polynuclear gold(I) sulfido complexes. For the first time, a mixture of both the decanuclear and dodecanuclear gold(I) complexes was obtained. Moreover, one of the dodecanuclear gold(I) complexes shows an unprecedented concentration-dependent cluster-to-cluster transformation, in which the two clusters of dodeca- and hexanuclear identities could be interconverted by changing the concentration of the complex. This work has provided a simple approach to bring about a structural modulation of gold(I) sulfido complexes by fine-tuning the substituent groups of the PNP ligands. The occurrence of the interconversion has provided a system for the study and understanding of supramolecular transformations in polynuclear gold(I) systems under the application of external stimuli.

ASSOCIATED CONTENT

Supporting Information

The Supporting Information is available free of charge at https://pubs.acs.org/doi/10.1021/jacs.0c04677.

General synthesis and characterization, X-ray crystallography, photophysical properties, and supplementary figures (PDF)

Crystal data for $\mathbf{L^{Et}}$-$\mathbf{Au_{10}}$ (CIF)

Crystal data for $\mathbf{L^{Me}}$-$\mathbf{Au_{10}}$ (CIF)

Crystal data for $\mathbf{L^{Me}}$-$\mathbf{Au_{12}}$ (CIF)

Crystal data for $\mathbf{L^{H}}$-$\mathbf{Au_{12}}$ (CIF)

https://dx.doi.org/10.1021/jacs.0c04677
J. Am. Chem. Soc. XXXX, XXX, XXX−XXX

AUTHOR INFORMATION

Corresponding Author

Vivian Wing-Wah Yam − *Institute of Molecular Functional Materials and Department of Chemistry, The University of Hong Kong, Hong Kong, P. R. China;* orcid.org/0000-0001-8349-4429; Email: wwyam@hku.hk

Authors

Liang-Liang Yan − *Institute of Molecular Functional Materials and Department of Chemistry, The University of Hong Kong, Hong Kong, P. R. China;* orcid.org/0000-0001-5210-1645

Liao-Yuan Yao − *Institute of Molecular Functional Materials and Department of Chemistry, The University of Hong Kong, Hong Kong, P. R. China;* orcid.org/0000-0003-2119-3895

Complete contact information is available at: https://pubs.acs.org/10.1021/jacs.0c04677

Notes

The authors declare no competing financial interest.

ACKNOWLEDGMENTS

V.W.-W.Y. acknowledges UGC funding administered by The University of Hong Kong for supporting the Electrospray Ionization Quadrupole Time-of-Flight Mass Spectrometry Facilities under the Support for Interdisciplinary Research in Chemical Science and the support from The University of Hong Kong under the University Research Committee (URC) Strategically Oriented Research Theme (SORT) on Functional Materials for Molecular Electronics. This work has been supported by the Key Program of the Major Research Plan on "Architectures, Functionalities and Evolution of Hierarchical Clusters" of the National Natural Science Foundation of China (Grant no. 91961202) and a General Research Fund (GRF) from the Research Grants Council of Hong Kong Special Administrative Region, P. R. China (HKU17301517). L.-L.Y. acknowledges the receipt of a postgraduate studentship from The University of Hong Kong. The Beijing Synchrotron Radiation Facility (BSRF) is also acknowledged for providing beamline time of the synchrotron radiation X-ray diffraction facilities. We also thank the staff of BL17B beamline at the National Facility for Protein Science (NFPS) of the Shanghai Synchrotron Radiation Facility (SSRF), Shanghai, P. R. China, for assistance during data collection. We also thank Dr. Michael Ho-Yeung Chan, Dr. Anlea Chu, and Dr. Desmond Yat-Hin Cheng for CSI-MS data collection.

REFERENCES

(1) Wang, W.; Wang, Y.-X.; Yang, H.-B. Supramolecular Transformations within Discrete Coordination-driven Supramolecular Architectures. *Chem. Soc. Rev.* **2016**, *45*, 2656−2693.

(2) McConnell, A. J.; Wood, C. S.; Neelakandan, P. P.; Nitschke, J. R. Stimuli-Responsive Metal−Ligand Assemblies. *Chem. Rev.* **2015**, *115*, 7729−7793.

(3) Betancourt, J. E.; Martín-Hidalgo, M.; Gubala, V.; Rivera, J. M. Solvent-Induced High Fidelity Switching Between Two Discrete Supramolecules. *J. Am. Chem. Soc.* **2009**, *131*, 3186−3188.

(4) Dublin, S. N.; Conticello, V. P. Design of a Selective Metal Ion Switch for Self-Assembly of Peptide-Based Fibrils. *J. Am. Chem. Soc.* **2008**, *130*, 49−51.

(5) Fujita, M.; Ibukuro, F.; Seki, H.; Kamo, O.; Imanari, M.; Ogura, K. Catenane Formation from Two Molecular Rings through Very Rapid Slippage. A Möbius Strip Mechanism. *J. Am. Chem. Soc.* **1996**, *118*, 899−900.

(6) Gu, Y.; Alt, E. A.; Wang, H.; Li, X.; Willard, A. P.; Johnson, J. A. Photoswitching Topology in Polymer Networks with Metal−organic Cages as Crosslinks. *Nature* **2018**, *560*, 65−69.

(7) Yamamoto, T.; Arif, A. M.; Stang, P. J. Dynamic Equilibrium of a Supramolecular Dimeric Rhomboid and Trimeric Hexagon and Determination of Its Thermodynamic Constants. *J. Am. Chem. Soc.* **2003**, *125*, 12309−12317.

(8) Heo, J.; Jeon, Y.-M.; Mirkin, C. A. Reversible Interconversion of Homochiral Triangular Macrocycles and Helical Coordination Polymers. *J. Am. Chem. Soc.* **2007**, *129*, 7712−7713.

(9) Liu, T.-F.; Chen, Y.-P.; Yakovenko, A. A.; Zhou, H.-C. Interconversion between Discrete and a Chain of Nanocages: Self-Assembly via a Solvent-Driven, Dimension-Augmentation Strategy. *J. Am. Chem. Soc.* **2012**, *134*, 17358−17361.

(10) Lu, X.; Li, X.; Guo, K.; Xie, T.-Z.; Moorefield, C. N.; Wesdemiotis, C.; Newkome, G. R. Probing a Hidden World of Molecular Self-Assembly: Concentration-Dependent, Three-Dimensional Supramolecular Interconversions. *J. Am. Chem. Soc.* **2014**, *136*, 18149−18155.

(11) Ramírez, J.; Stadler, A.-M.; Kyritsakas, N.; Lehn, J.-M. Solvent-modulated Reversible Conversion of a [2 × 2]-grid into a Pincer-like Complex. *Chem. Commun.* **2007**, 237−239.

(12) Raymo, F. M.; Houk, K. N.; Stoddart, J. F. Origins of Selectivity in Molecular and Supramolecular Entities: Solvent and Electrostatic Control of the Translational Isomerism in [2]Catenanes. *J. Org. Chem.* **1998**, *63*, 6523−6528.

(13) Sautter, A.; Schmid, D. G.; Jung, G.; Würthner, F. A Triangle−Square Equilibrium of Metallosupramolecular Assemblies Based on Pd(II) and Pt(II) Corners and Diazadibenzoperylene Bridging Ligands. *J. Am. Chem. Soc.* **2001**, *123*, 5424−5430.

(14) Li, M.; Chen, L.-J.; Cai, Y.; Luo, Q.; Li, W.; Yang, H.-B.; Tian, H.; Zhu, W.-H. Light-Driven Chiral Switching of Supramolecular Metallacycles with Photoreversibility. *Chem.* **2019**, *5*, 634−648.

(15) McTernan, C. T.; Ronson, T. K.; Nitschke, J. R. Post-assembly Modification of Phosphine Cages Controls Host−Guest Behavior. *J. Am. Chem. Soc.* **2019**, *141*, 6837−6842.

(16) Xu, G.-T.; Wu, L.-L.; Chang, X.-Y.; Ang, T. W. H.; Wong, W.-Y.; Huang, J.-S.; Che, C.-M. Solvent-Induced Cluster-to-Cluster Transformation of Homoleptic Gold(I) Thiolates between Catenane and Ring-in-Ring Structures. *Angew. Chem., Int. Ed.* **2019**, *58*, 16297−16306.

(17) Zheng, W.; Wang, W.; Jiang, S.-T.; Yang, G.; Li, Z.; Wang, X.-Q.; Yin, G.-Q.; Zhang, Y.; Tan, H.; Li, X.; Ding, H.; Chen, G.; Yang, H.-B. Supramolecular Transformation of Metallacycle-linked Star Polymers Driven by Simple Phosphine Ligand-Exchange Reaction. *J. Am. Chem. Soc.* **2019**, *141*, 583−591.

(18) Scherbaum, F.; Grohmann, A.; Huber, B.; Krüger, C.; Schmidbaur, H. "Aurophilicity" as a Consequence of Relativistic Effects: The Hexakis(triphenylphosphaneaurio)methane Dication $[(Ph_3PAu)_6C]^{2\oplus}$. *Angew. Chem., Int. Ed. Engl.* **1988**, *27*, 1544−1546.

(19) Schmidbaur, H. Ludwig Mond Lecture. High-carat Gold Compounds. *Chem. Soc. Rev.* **1995**, *24*, 391−400.

(20) Schmidbaur, H.; Schier, A. A Briefing on Aurophilicity. *Chem. Soc. Rev.* **2008**, *37*, 1931−1951.

(21) Schmidbaur, H.; Schier, A. Aurophilic Interactions as a Subject of Current Research: an Up-date. *Chem. Soc. Rev.* **2012**, *41*, 370−412.

(22) Balch, A. L.; Olmstead, M. M.; Vickery, J. C. Gold(I) Compounds without Significant Aurophilic Intermolecular Interactions: Synthesis, Structure, and Electronic Properties of $Ph_3PAuC(O)NHMe$ and $Au_3(PhCH_2NCOMe)_3$: Comparative Monomeric and Trimeric Analogues of the Solvoluminescent Trimer, $Au_3(MeNCOMe)_3$. *Inorg. Chem.* **1999**, *38*, 3494−3499.

(23) Brandys, M.-C.; Puddephatt, R. J. Strongly Luminescent Three-Coordinate Gold(I) Polymers: 1D Chain-Link Fence and 2D Chickenwire Structures. *J. Am. Chem. Soc.* **2001**, *123*, 4839−4840.

(24) Canales, F.; Gimeno, M. C.; Laguna, A.; Jones, P. G. Aurophilicity at Sulfur Centers. Synthesis and Reactivity of the Complex $[S(Au_2dppf)]$; Formation of Polynuclear Sulfur-Centered Complexes. Crystal Structures of $[S(Au_2dppf)]\cdot 2CHCl_3$, $[(\mu$-

https://dx.doi.org/10.1021/jacs.0c04677
J. Am. Chem. Soc. XXXX, XXX, XXX−XXX

$Au_2dppf\{S(Au_2dppf)\}_2](OTf)_2\cdot 8CHCl_3$, and [S-$(AuPPh_2Me)_2(Au_2dppf)](ClO_4)_2\cdot 3CH_2Cl_2$. *J. Am. Chem. Soc.* **1996**, *118*, 4839−4845.
(25) Chen, J.; Mohamed, A. A.; Abdou, H. E.; Krause Bauer, J. A.; Fackler, J. P., Jr.; Bruce, A. E.; Bruce, M. R. M. Novel metallamacrocyclic gold(I) thiolate cluster complex: structure and luminescence of $[Au_9(\mu\text{-dppm})_4(\mu\text{-p-tc})_6](PF_6)_3$. *Chem. Commun.* **2005**, 1575−1577.
(26) Cheng, E. C.-C.; Lo, W.-Y.; Lee, T. K.-M.; Zhu, N.; Yam, V. W.-W. Synthesis, Characterization, and Luminescence Studies of Discrete Polynuclear Gold(I) Sulfido and Selenido Complexes with Intramolecular Aurophilic Contacts. *Inorg. Chem.* **2014**, *53*, 3854−3863.
(27) Chui, S. S.-Y.; Chen, R.; Che, C.-M. A Chiral [2]Catenane Precursor of the Antiarthritic Gold(I) Drug Auranofin. *Angew. Chem., Int. Ed.* **2006**, *45* (10), 1621−1624.
(28) Fenske, D.; Langetepe, T.; Kappes, M. M.; Hampe, O.; Weis, P. Selenium-Bridged Gold(I) Complex Cations $[Au_{10}Se_4(dppm)_4]^{2+}$ and $[Au_{18}Se_8(dppe)_6]^{2+}$. *Angew. Chem., Int. Ed.* **2000**, *39*, 1857−1860.
(29) Fung, E. Y.; Olmstead, M. M.; Vickery, J. C.; Balch, A. L. Glowing Gold Rings: Solvoluminescence from Planar Trigold(I) Complexes. *Coord. Chem. Rev.* **1998**, *171*, 151−159.
(30) Gimeno, M. C.; Laguna, A. Three- and Four-Coordinate Gold(I) Complexes. *Chem. Rev.* **1997**, *97*, 511−522.
(31) Gimeno, M. C.; Laguna, A. Chalcogenide Centred Gold Complexes. *Chem. Soc. Rev.* **2008**, *37*, 1952−1966.
(32) He, X.; Yam, V. W.-W. Luminescent Gold(I) Complexes for Chemosensing. *Coord. Chem. Rev.* **2011**, *255*, 2111−2123.
(33) Jia, J.-H.; Wang, Q.-M. Intensely Luminescent Gold(I)−Silver(I) Cluster with Hypercoordinated Carbon. *J. Am. Chem. Soc.* **2009**, *131*, 16634−16635.
(34) Jiang, X.-F.; Hau, F. K.-W.; Sun, Q.-F.; Yu, S.-Y.; Yam, V. W.-W. From $\{Au^I\cdots Au^I\}$-Coupled Cages to the Cage-Built 2-D $\{Au^I\cdots Au^I\}$ Arrays: $Au^I\cdots Au^I$ Bonding Interaction Driven Self-Assembly and Their Ag^I Sensing and Photo-Switchable Behavior. *J. Am. Chem. Soc.* **2014**, *136*, 10921−10929.
(35) Katz, M. J.; Sakai, K.; Leznoff, D. B. The Use of Aurophilic and Other Metal−metal Interactions as Crystal Engineering Design Elements to Increase Structural Dimensionality. *Chem. Soc. Rev.* **2008**, *37*, 1884−1895.
(36) Koshevoy, I. O.; Chang, Y.-C.; Karttunen, A. J.; Haukka, M.; Pakkanen, T.; Chou, P.-T. Modulation of Metallophilic Bonds: Solvent-Induced Isomerization and Luminescence Vapochromism of a Polymorphic Au−Cu Cluster. *J. Am. Chem. Soc.* **2012**, *134*, 6564−6567.
(37) Lasanta, T.; Olmos, M. E.; Laguna, A.; López-de-Luzuriaga, J. M.; Naumov, P. Making the Golden Connection: Reversible Mechanochemical and Vapochemical Switching of Luminescence from Bimetallic Gold−Silver Clusters Associated through Aurophilic Interactions. *J. Am. Chem. Soc.* **2011**, *133*, 16358−16361.
(38) Lee, Y.-A.; Eisenberg, R. Luminescence Tribochromism and Bright Emission in Gold(I) Thiouracilate Complexes. *J. Am. Chem. Soc.* **2003**, *125*, 7778−7779.
(39) Lim, S. H.; Olmstead, M. M.; Balch, A. L. Molecular Accordion: Vapoluminescence and Molecular Flexibility in the Orange and Green Luminescent Crystals of the Dimer, $Au_2(\mu\text{-bis-(diphenylphosphino)ethane})_2Br_2$. *J. Am. Chem. Soc.* **2011**, *133*, 10229−10238.
(40) Lim, S. H.; Olmstead, M. M.; Balch, A. L. Inorganic topochemistry. Vapor-induced Solid State Transformations of Luminescent, Three-coordinate Gold(I) Complexes. *Chem. Sci.* **2013**, *4*, 311−318.
(41) Manbeck, G. F.; Brennessel, W. W.; Stockland, R. A.; Eisenberg, R. Luminescent Au(I)/Cu(I) Alkynyl Clusters with an Ethynyl Steroid and Related Aliphatic Ligands: An Octanuclear Au_4Cu_4 Cluster and Luminescence Polymorphism in Au_3Cu_2 Clusters. *J. Am. Chem. Soc.* **2010**, *132*, 12307−12318.
(42) Ni, W.-X.; Li, M.; Zheng, J.; Zhan, S.-Z.; Qiu, Y.-M.; Ng, S. W.; Li, D. Approaching White-Light Emission from a Phosphorescent Trinuclear Gold(I) Cluster by Modulating Its Aggregation Behavior. *Angew. Chem., Int. Ed.* **2013**, *52*, 13472−13476.
(43) Polgar, A. M.; Weigend, F.; Zhang, A.; Stillman, M. J.; Corrigan, J. F. A N-Heterocyclic Carbene-Stabilized Coinage Metal-Chalcogenide Framework with Tunable Optical Properties. *J. Am. Chem. Soc.* **2017**, *139*, 14045−14048.
(44) Puddephatt, R. J. Coordination Polymers: Polymers, Rings and Oligomers Containing Gold(I) Centres. *Coord. Chem. Rev.* **2001**, *216*, 313−332.
(45) Puddephatt, R. J. Macrocycles, Catenanes, Oligomers and Polymers in Gold Chemistry. *Chem. Soc. Rev.* **2008**, *37*, 2012−2027.
(46) Rawashdeh-Omary, M. A.; Omary, M. A.; Fackler, J. P.; Galassi, R.; Pietroni, B. R.; Burini, A. Chemistry and Optoelectronic Properties of Stacked Supramolecular Entities of Trinuclear Gold(I) Complexes Sandwiching Small Organic Acids. *J. Am. Chem. Soc.* **2001**, *123*, 9689−9691.
(47) Siemeling, U.; Rother, D.; Bruhn, C.; Fink, H.; Weidner, T.; Träger, F.; Rothenberger, A.; Fenske, D.; Priebe, A.; Maurer, J.; Winter, R. The Interaction of 1,1′-Diisocyanoferrocene with Gold: Formation of Monolayers and Supramolecular Polymerization of an Aurophilic Ferrocenophane. *J. Am. Chem. Soc.* **2005**, *127*, 1102−1103.
(48) Wang, Q.-M.; Lee, Y.-A.; Crespo, O.; Deaton, J.; Tang, C.; Gysling, H. J.; Concepción Gimeno, M.; Larraz, C.; Villacampa, M. D.; Laguna, A.; Eisenberg, R. Intensely Luminescent Gold(I)−Silver(I) Cluster Complexes with Tunable Structural Features. *J. Am. Chem. Soc.* **2004**, *126*, 9488−9489.
(49) Kilbas, B.; Mirtschin, S.; Scopelliti, R.; Severin, K. A Solvent-responsive Coordination Cage. *Chem. Sci.* **2012**, *3*, 701−704.
(50) Suzuki, K.; Kawano, M.; Fujita, M. Solvato-Controlled Assembly of Pd_3L_6 and Pd_4L_8 Coordination "Boxes". *Angew. Chem., Int. Ed.* **2007**, *46*, 2819−2822.
(51) Fujita, M. Self-Assembly of [2]Catenanes Containing Metals in Their Backbones. *Acc. Chem. Res.* **1999**, *32*, 53−61.
(52) Stephenson, A.; Argent, S. P.; Riis-Johannessen, T.; Tidmarsh, I. S.; Ward, M. D. Structures and Dynamic Behavior of Large Polyhedral Coordination Cages: An Unusual Cage-to-Cage Interconversion. *J. Am. Chem. Soc.* **2011**, *133*, 858−870.
(53) McPartlin, M.; Mason, R.; Malatesta, L. Novel Cluster Complexes of Gold(0)−Gold(I). *J. Chem. Soc. D* **1969**, *0*, 334−334.
(54) Briant, C. E.; Theobald, B. R. C.; White, J. W.; Bell, L. K.; Mingos, D. M. P.; Welch, A. J. Synthesis and X-ray Structural Characterization of the Centred Icosahedral Gold Cluster Compound $[Au_{13}(PMe_2Ph)_{10}Cl_2](PF_6)_3$; the Realization of a Theoretical Prediction. *J. Chem. Soc., Chem. Commun.* **1981**, 201−202.
(55) Teo, B. K.; Shi, X.; Zhang, H. Pure Gold Cluster of 1:9:9:1:9:9:1 Layered Structure: a Novel 39-Metal-Atom Cluster $[(Ph_3P)_{14}Au_{39}Cl_6]Cl_2$ with an Interstitial Gold Atom in a Hexagonal Antiprismatic Cage. *J. Am. Chem. Soc.* **1992**, *114*, 2743−2745.
(56) Menard, L. D.; Gao, S.-P.; Xu, H.; Twesten, R. D.; Harper, A. S.; Song, Y.; Wang, G.; Douglas, A. D.; Yang, J. C.; Frenkel, A. I.; Nuzzo, R. G.; Murray, R. W. Sub-Nanometer Au Monolayer-Protected Clusters Exhibiting Molecule-like Electronic Behavior: Quantitative High-Angle Annular Dark-Field Scanning Transmission Electron Microscopy and Electrochemical Characterization of Clusters with Precise Atomic Stoichiometry. *J. Phys. Chem. B* **2006**, *110*, 12874−12883.
(57) Angermaier, K.; Schmidbaur, H. The Supramolecular Structures of Complex Tri[Gold(I)]Sulfonium Cations. *Chem. Ber.* **1994**, *127*, 2387−2391.
(58) Canales, F.; Gimeno, C.; Laguna, A.; Villacampa, M. D. Aurophilicity at Sulfur Centers. Synthesis of the Polyaurated Species $[S(AuPR_3)_n]^{(n-2)+}$ (n = 2−6). *Inorg. Chim. Acta* **1996**, *244*, 95−103.
(59) Jones, P. G.; Sheldrick, G. M.; Hadicke, E. μ_3-Sulphido-Tris[triphenylphosphinegold(I)] Hexafluorophosphate. *Acta Crystallogr., Sect. B: Struct. Crystallogr. Cryst. Chem.* **1980**, *36*, 2777−2779.
(60) Chu, A.; Hau, F. K.-W.; Yao, L.-Y.; Yam, V. W.-W. Decanuclear Gold(I) Sulfido Pseudopolymorphs Displaying Stimuli-Responsive RGBY Luminescence Changes. *ACS Materials Lett.* **2019**, *1*, 277−284.

https://dx.doi.org/10.1021/jacs.0c04677
J. Am. Chem. Soc. XXXX, XXX, XXX−XXX

(61) Lee, T. K.-M.; Zhu, N.; Yam, V. W.-W. An Unprecedented Luminescent Polynuclear Gold(I) μ_3-Sulfido Cluster With a Thiacrown-like Architecture. *J. Am. Chem. Soc.* **2010**, *132*, 17646−17648.
(62) Yam, V. W.-W.; Cheng, E. C.-C. Molecular Gold—Multinuclear Gold(I) Complexes. *Angew. Chem., Int. Ed.* **2000**, *39*, 4240−4242.
(63) Yam, V. W.-W.; Cheng, E. C.-C.; Cheung, K.-K. A Novel High-Nuclearity Luminescent Gold(I)−Sulfido Complex. *Angew. Chem., Int. Ed.* **1999**, *38*, 197−199.
(64) Yam, V. W.-W.; Cheng, E. C.-C.; Zhou, Z.-Y. A Highly Soluble Luminescent Decanuclear Gold(I) Complex with a Propeller-Shaped Structure. *Angew. Chem., Int. Ed.* **2000**, *39*, 1683−1685.
(65) Yam, V. W.-W.; Cheng, E. C.-C.; Zhu, N. A Novel Polynuclear Gold−Sulfur Cube with an Unusually Large Stokes Shift. *Angew. Chem., Int. Ed.* **2001**, *40*, 1763−1765.
(66) Yao, L.-Y.; Hau, F. K.-W.; Yam, V. W.-W. Addition Reaction-Induced Cluster-to-Cluster Transformation: Controlled Self-Assembly of Luminescent Polynuclear Gold(I) μ_3-Sulfido Clusters. *J. Am. Chem. Soc.* **2014**, *136*, 10801−10806.
(67) Yao, L.-Y.; Lee, T. K.-M.; Yam, V. W.-W. Thermodynamic-Driven Self-Assembly: Heterochiral Self-Sorting and Structural Reconfiguration in Gold(I)−Sulfido Cluster System. *J. Am. Chem. Soc.* **2016**, *138*, 7260−7263.
(68) Yao, L.-Y.; Yam, V. W.-W. Photoinduced Isomerization-Driven Structural Transformation Between Decanuclear and Octadecanuclear Gold(I) Sulfido Clusters. *J. Am. Chem. Soc.* **2015**, *137*, 3506−3509.
(69) Yao, L.-Y.; Low, K.-H.; Yam, V. W.-W. A Gold Quartet Framework with Reversible Anisotropic Structural Transformation Accompanied by Luminescence Response. *Chem.* **2019**, *5*, 2418−2428.
(70) Yam, V. W.-W.; Au, V. K.-M.; Leung, S. Y.-L. Light-Emitting Self-Assembled Materials Based on d^8 and d^{10} Transition Metal Complexes. *Chem. Rev.* **2015**, *115*, 7589−7728.

https://dx.doi.org/10.1021/jacs.0c04677
J. Am. Chem. Soc. XXXX, XXX, XXX−XXX